

EFFECT OF K, Co AND Mo ADDITION IN Fe-BASED CATALYSTS FOR AVIATION BIOFUELS PRODUCTION BY FISCHER-TROPSCH SYNTHESIS

D. Martínez, C. Martos, J. Dufour, A.J. Vizcaíno
Chemical and Environmental Engineering Group, Rey Juan Carlos University, Madrid, Spain
Corresponding author: Daniel Martínez, daniel.delmonte@urjc.es

REFERENCE NO	ABSTRACT
BIOF-05	In the search for environmentally friendly solutions to produce clean fuels, Fischer-Tropsch Synthesis arises as a promising alternative where syngas obtained from biomass is transformed into hydrocarbons such as kerosene. Fe-based catalysts are typically used in this process. Addition of chemical promoters can improve the activity of these catalysts. Thus, in this work, Fe-based catalysts were prepared by precipitation of iron oxides and the subsequent addition of K (3% wt %), Mo and Co (6 wt %) by impregnation. Catalytic tests were carried out for 60h at 250 °C and 20 bar in a fixed-bed reactor using diluted syngas with a H ₂ :CO:N ₂ molar ratio of 6:3:1. The addition of K and Co stabilizes catalytic activity, while the selectivity to kerosene range hydrocarbon is increased. In addition, Co and K co-promoted catalyst reached the highest CO conversion and kerosene selectivity.
<i>Keywords:</i> Fischer-Tropsch synthesis Iron catalysts Kerosene Aviation biofuel	

1. INTRODUCTION

An increase of 50% in the worldwide fuels production is estimated by 2040 to satisfy the transportation energy requirements. Concretely, kerosene-type jet fuel is planned to be doubled for the same period [1]. Currently the economy of transportation is based on hydrocarbons from oil. Due to the high concern about fossil resources depletion and the global warming because of the rise of CO₂ level in the atmosphere, it is mandatory to find a sustainable and environmentally friendly alternative [2]. While road transports could run on with alternative fuels than biofuels, such as green electricity, this will not be an option for aviation where kerosene will be required- [3]. In this, mean Fischer-Tropsch synthesis (FTS) could be an alternative to produce synthetic clean liquid fuels for transportation. FTS is a key gas-to-liquids (GTLs) technology to produce synthetic fuels by syngas (CO + H₂) transformation[4,5]. Moreover, syngas can be obtained from renewable resources as biomass through various different pathways. This technology, which transforms biomass into liquid fuels, is called Biomass-to-Liquids (BTL). The H₂/CO stream can be produced by biomass gasification [6] or even steam

reforming of biomass-derived liquids [7,8] and the H₂/CO ratio can be adjusted then by WGS in a membrane reactor [9].

The choice of an appropriate catalyst according to different parameters, such as the required product, the price of the catalyst, the syngas composition or possible refining processes after reaction is an important issue [10]. Although some metals of groups 8-10 (Fe, Ru, Co and Ni) exhibit good catalytic properties in FTS, Fe-based catalysts are usually a good choice due to its low cost, adjustable selectivity and its water-gas shift (WGS) activity, which allows a flexible H₂/CO ratio [11]. Addition of promoters is a common practise to improve the catalytic activity and stability as well as the selectivity tuning. Several metals have been studied as Fe-based promoters in order to improve catalytic activity by increasing its reducibility, preventing the catalyst deactivation or enhancing the active surface of catalysts [12]. Nevertheless, there are no several studies about promoted Fe-based catalyst to maximize the kerosene yield production (C₉-C₁₆). Promoters such as potassium has been widely used in order to decrease the selectivity to CH₄ enhancing the selectivity to heavier products. Potassium can also improve the

activity in FTS and WGS reactions [12][13]. Cobalt is an active metal itself in the FTS. Although few studies can be found about cobalt as an iron catalysts promoter for FTS, the Fe-Co alloy has been reported to exhibit good activity and selectivity [14–16]. On the other hand, the addition of molybdenum as promoter of FTS iron catalysts has generated controversy since, while some authors suggest that Mo enhances the FTS performance [11,12], other studies report the formation of a reduction resistant phase ($\text{Fe}_2(\text{MoO}_4)_3$) which inhibits the active phase formation during the catalyst activation [19]. Thus, the purpose of this study was to investigate the effect of K, Mo and Co addition to Fe-based catalysts for kerosene production by FTS.

2. EXPERIMENTAL

2.1. Catalysts preparation

In this study, the promoted iron catalysts were synthesised using the following procedure. Iron oxide precursor was precipitated from an iron nitrate solution prepared by solving $\text{Fe}(\text{NO}_3)_3 \cdot 9\text{H}_2\text{O}$ in milliQ grade water by adding aqueous solution of NH_4OH (2M) as precipitation agent. The ferritic nitrate solution was heated up to $80^\circ \pm 1^\circ\text{C}$ in a beaker under continuous stirring. The NH_4OH solution was added dropwise over the hot iron nitrate solution until it reached a constant pH value of 8 ± 0.1 . Then the solution was aged for 60 min. The iron precipitate was then filtered, washed, dried at 110°C for 24h and finally calcined at 450°C for 4h. Potassium-, cobalt- and molybdenum-promoted catalysts were prepared by impregnation using KNO_3 , $\text{CoN}_2\text{O}_6 \cdot 6\text{H}_2\text{O}$ and $(\text{NH}_4)_6\text{Mo}_7\text{O}_{24} \cdot 4\text{H}_2\text{O}$ aqueous solutions, respectively, with the proper amount of K, Co and Mo to reach a 3 wt % of K content and a 6% of Co and Mo content in the final catalysts. The resulting samples were calcined under air atmosphere at 450°C for 4h. The prepared catalysts were denoted as Fe, FeK, FeMo, FeCo, FeKMo and FeKCo depending on the promoter added.

2.2. Catalysts characterization

The metal composition of the prepared materials was measured by *X-ray fluorescence* (XRF) using a Philips Magix spectrometer. Previously, a calibration was performed using samples with known chemical composition.

N₂-adsorption-desorption measurements were carried out at 77K using a Quantachrome Nova 4000 analyzer. Catalysts surface areas were calculated using the BET method.

X-Ray diffraction (XRD) measurements were carried using a Philips Xpert Pro MPD/MRD system in the 2θ range from 10 to 70° with a step size of 0.02° , using a Cu K_α radiation source. Crystalline phases were identified according to patterns from the JCPDS index.

The structure and morphology of the fresh catalysts were observed by *scanning electron microscopy* (SEM) using a Philips XL30 ESEM microscope operated at 200 kV.

Temperature programmed reduction (TPR) analyses were carried out to determine the reducibility of the calcined catalysts. Measurements were performed in a Micrometrics Autochem 2910 equipment under 10% H_2 in Ar flow using a heating rate of $10^\circ\text{C}/\text{min}$ from 25 to 1000°C . Samples were previously degassed under dry Ar flow at 120°C .

2.3. Catalytic tests

Catalytic tests were carried out in a Microactivity Reference unit (PID Eng & Tech). The system consists of an automatized stainless steel fixed-bed tubular reactor (internal diameter: 9 mm; length: 300 mm) located inside an electric oven. The catalyst (0.5g) was diluted in SiC (1.5g) to avoid hot spots during the reaction and then it was placed inside the reactor. Prior to the catalytic test, samples were reduced in situ by syngas (H_2/CO ratio =2) at 350°C , atmospheric pressure and $3\text{Nl/g}\cdot\text{h}$ space velocity for 10h. In addition, undiluted samples were reduced following this procedure in order to be characterized. After the activation period, the reactor was led to reaction conditions under

N₂ flow. FTS tests were carried out at 20bar and 250°C, feeding a H₂:CO:N₂ mixture with 6:3:1 molar ratio at 3Nl/g·h space velocity for 60h. The reactor effluent passed through a hot trap (100°C) to collect heavy waxes and a cold trap (0°C) to recover light waxes and water. The gaseous product stream was continuously analysed on-line with a Varian CP-4900 Micro-GC equipped with Molecular Sieve 5A and Poraplot Q columns and a TCD. Light waxes and water were separated by decantation and the organic liquid mixture was analysed off-line in a Varian 3800 GC, equipped with an Agilent DB-200 column and FID.

3. RESULTS AND DISCUSSION

3.1. Fresh catalysts characterization

The metal composition, determined by XRD, and the BET surface area of the calcined samples are shown in Table 1. The results confirm that K, Mo and Co loadings are close to the desired content.

Table 1. Metal content and BET surface area of the calcined Fe-based catalysts.

Catalyst	XRF metal composition (wt%)				BET surface area (m ² /g)
	Fe	K	Mo	Co	
Fe	100.0	0.0	0.0	0.0	20.6
FeK	97.8	2.2	0.0	0.0	17.7
FeMo	93.1	0.0	6.9	0.0	22.2
FeCo	91.9	0.0	0.0	8.1	21.9
FeKMo	88.8	3.8	7.4	0.0	11.6
FeKCo	82.7	1.7	0.0	7.5	8.9

According to Table 1, samples exhibit similar surface areas (~ 20 m²), except for those with two promoters (FeKMo and FeKCo), which lower specific surfaces.

The XRD patterns of the calcined catalysts are illustrated in Fig. 1. Diffraction peaks corresponding to hematite (α -Fe₂O₃) can be observed at 24.2, 33.1, 35.6, 40.8, 49.5, 54.0, 57.6, 62.5 and 64.0° in all cases. No diffraction line corresponding to additional K,

Mo or Co phases were detected. Besides, the presence of promoters did not seem to affect the intensity of hematite diffraction.

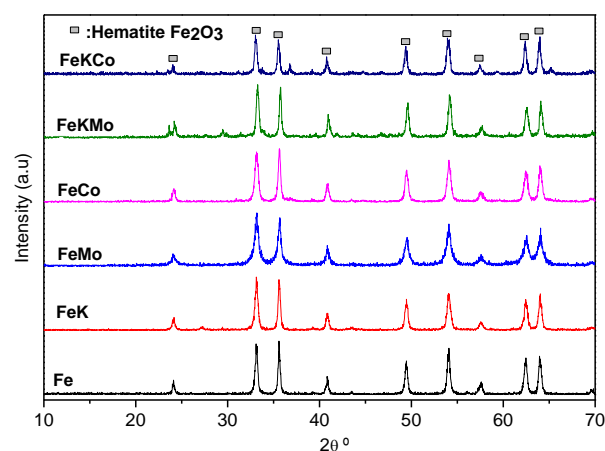


Fig. 1. XRD patterns of Fe-based catalysts before reaction.

The morphological properties of fresh catalysts were analysed by SEM as shown in Figure 2. All the prepared Fe-based catalysts exhibit an irregular morphology with a wide particles size distribution, ranging from 1 to 100µm.

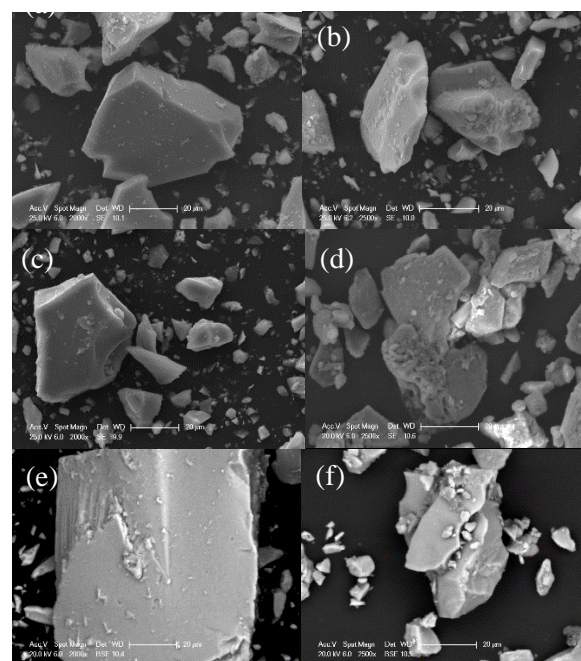


Fig. 2. SEM images of the fresh catalyst: (a) Fe; (b) FeK; (c) FeMo ; (d) FeCo; (e) FeKMo and (f) FeKCo

The distribution of promoting elements on the catalysts was analysed by means of Energy Dispersive X-Ray Microanalysis (EDX). The added promoters were homogeneously

dispersed on the catalysts particles in all cases (not shown).

H₂-TPR was used to determine the effect of the different promoters on the Fe-based catalysts reducibility and the corresponding profiles are shown in Fig.3. Unpromoted iron catalyst (Fig. 3a) shows a typical iron oxide reduction behaviour where the first peak at 379°C corresponds to Fe₂O₃ → Fe₃O₄ transformation and the peak at higher temperature (around 670°C) includes the Fe₃O₄ → FeO → Fe reductions. FeK catalyst (Fig. 3b) exhibits a similar TPR profile, but reduction features are shifted to higher temperatures in comparison to the unpromoted sample (457 and 719 °C), according to the reported effect of K to stabilize Fe₂O₃ against reduction [20]. However, the profile of FeMo (Fig. 3c) shows reduction peaks at much higher temperatures with a first reduction feature at 538°C, attributed to hematite conversion to Fe₃O₄ and a second broad reduction zone around 800 °C. This profile suggests that Mo inhibits the reduction of Fe-based catalysts. According to literature [15,16], the activation energy of the reduction MoO₃ → MoO₂ is higher than that of Fe₂O₃ → Fe₃O₄. So, removal of O atoms from iron phase during the reduction is avoided due to the worse reducibility of molybdenum oxide that might cover the iron phase. On the other hand, some authors suggest the formation of ferric molybdate, Fe₂(MoO₄)₃, when the mixture Fe₂O₃ and MoO₃ is calcined [19]. Although ferric molybdate was not observed by XRD, the H₂-TPR and FTS test results (see section 3.3) are consistent with the presence of this phase, which has reduction temperatures higher than those of iron or molybdenum oxides. On the other hand, addition of cobalt to iron oxide in FeCo sample did not have significant effect in reduction temperatures (Fig. 3d). The first peak can be assigned to the reduction of Fe₂O₃ to Fe₃O₄ and Co₃O₄ to CoO, while signals at 570°C and 670°C correspond to the reduction of CoO to Co and Fe₃O₄ to Fe, respectively. Regarding the reduction behaviour of samples containing two promoters, FeKMo catalyst (Fig. 3e) exhibited higher reduction

temperatures than the unpromoted Fe sample due to the presence of both K and Mo, which have a negative effect on the iron oxides reducibility, leading to a reduction behaviour between FeK and FeMo samples. In fact, the catalyst is not completely reduced up to 1000°C. Similarly, FeKCo catalyst (Fig. 3f) shows a reduction behaviour intermediate between FeK and FeCo samples.

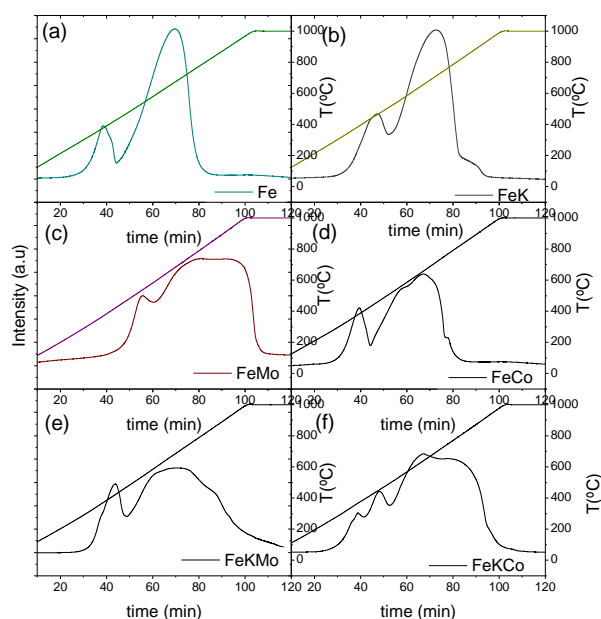


Fig. 3. H₂ TPR profiles of the fresh catalysts.

3.2 Characterization of catalysts after reduction under H₂/CO.

All catalysts were reduced following the activation procedure described in Section 2.3 and then analysed by XRD. The corresponding patterns are shown in Fig 4. Iron carbide phases were detected in the diffractograms of all catalysts, except for the FeKMo sample. No K, Mo, Co or Fe phases could be identified. Fe₂O₃ seems to be transformed to Fe or iron carbide during reduction with syngas. Fe is not detected due to the high reactivity of metallic iron with carbon dissociated from CO to form iron carbide [23]. Fe₅C₂ characteristic peaks at 35.8, 36.9, 39.5, 40.8, 43.5, 44.3, 45, 47.2, 50.6 and 58.6° were detected in FeKCo and FeCo patterns. Iron carbides as Fe₅C₂, Fe₂C or Fe₃C typically shows diffraction peaks at 2θ range between 30 and 60°. The diffraction

peaks around 35 and 60° in Fig. 4 are broad and it is difficult to identify all the types of iron carbides due to their poor crystallographic form. Some authors suggest that the formation of iron carbide is necessary to obtain significant FTS activity, the reaction activity depending on the surface area of carbide [24]. On the other hand, FeKMo diffraction pattern shows characteristic diffraction peaks of magnetite (Fe_3O_4), which indicates that this sample was unable to be properly reduced under the activation procedure used in this work due to its hard reducibility, as determined by H_2 -TPR

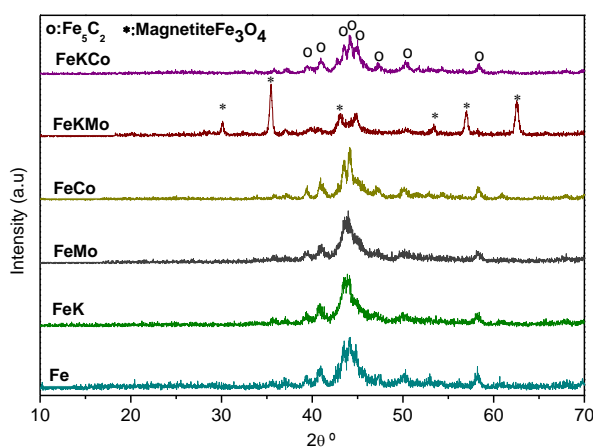


Fig. 4. XRD patterns of Fe-based catalysts after activation under H_2/CO .

3.3 Catalytic performance on FTS

3.3.1 Activity and stability

Fig. 5 shows the CO conversions of the prepared catalysts for the FTS reaction at 250°C and 20bar during 60h. Unpromoted Fe sample reached 70% of CO conversion in the first hours of reaction but then it decreases to 55 % and keeps almost constant at this value. Addition of Mo inhibited the FTS activity. In the case of the FeMo sample, the activity decreased to a 14% after the induction period and slightly increased with time on stream (TOS) up to 18%. Despite the presence of iron carbide after the activation step, the hard reducibility of this catalyst, determined by TPR, may hinder it to maintain the active species under reaction conditions. Besides, the FeKMo catalyst was not active. As explained

in Section 3.2, the reduction conditions were not effective enough to transform Fe_2O_3 to Fe (or iron carbide) and the catalyst remains as inactive Fe_3O_4 .

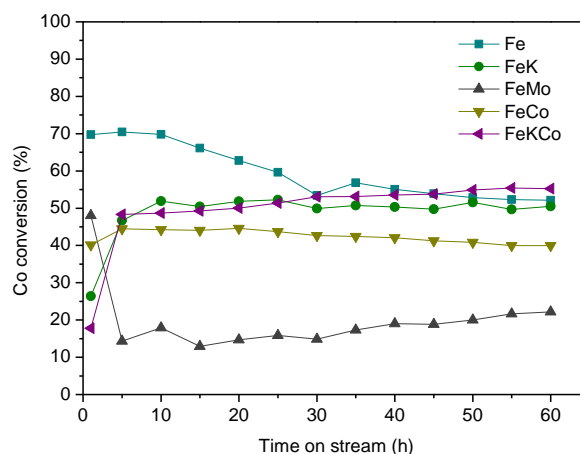


Fig. 5. Evolution in CO conversion in FTS using Fe-based catalysts.

On the other hand, FeK and FeKCo catalysts reached CO conversions similar to the unpromoted sample, slightly higher after 60h TOS in the case of the FeKCo sample. They show a 5-hour induction period after which the CO conversion remains almost constant. It seems that K is able to stabilize catalyst activity.

Finally, addition of Co also stabilized activity although with a lower conversion than the above discussed samples. Other works suggest the positive catalytic effect of combining Fe and Co in FTS supported catalysts [14]. The different behaviour found in the present work for these materials might be related to the differences in catalyst composition, preparation and in the absence of support in our study. Summing up, FeKCo catalyst exhibited the best activity results. CO conversion increased slowly during TOS reaching higher values than that of unpromoted iron catalyst after 60h. It has been reported that the presence of cobalt inhibits the formation of Fe_3O_4 from metallic iron and tends to form iron carbides during activation and reaction [25].

3.3.2 Product selectivity.

Iron based catalysts led to the formation different hydrocarbons that were divided in different groups for further study. They were grouped in light hydrocarbons (C₁-C₄), gasoline range (C₅-C₈), kerosene range (C₉-C₁₆) and heavy wax (C₁₇₊). Fig 6. illustrates that all active catalysts produced high yields of light hydrocarbons (methane mostly). Heat and mass transfers limitations are reported in literature as a possible reason for high methane yield by the formation of hot spots [26–28]. Regarding the catalytic promoters effect in the kerosene production selectivity. The addition of Mo not only leads to a decrease in the catalytic activity, but it also increased CH₄ production, with a consequent reduction in the production of higher-molecular-weight hydrocarbons. FeKMo was completely inactive so hydrocarbons were not detected in the product streams. These results are consistent with those found in literature [17]. The addition of K decreased the amount of methane produced, increasing the kerosene formation compared to that for Fe. It has been reported that alkali promoters, may improve CO dissociative adsorption, that facilitate chain growth reaction, so enhancing selectivity to heavy hydrocarbons [29]. Thus, it is reported that FTS can be set toward kerosene cut by using catalysts with low potassium content at low pressure (20 atm) [30]. FeCo has similar catalytic behaviour than FeK. It achieved also higher selectivity towards higher-molecular-weight hydrocarbons. This result is in agreement with other studies [31].

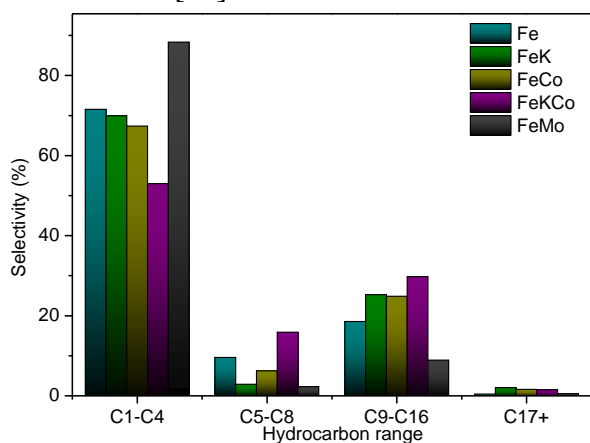


Fig. 6. Selectivity of CO with carbon number for each catalyst.

The addition of K and Co resulted in the lowest gaseous hydrocarbon fraction formation and the highest kerosene range hydrocarbons production. In addition, it also increased the gasoline range hydrocarbon selectivity. Although this cut is not the subject of this study, this fact is interesting due to the high value of this hydrocarbon range.

3.4 Characterization of catalysts after reaction.

The powder diffractograms of the used catalyst are shown in Fig. 7. Phase identification in used catalysts by XRD is hindered by the presence of high intensity SiC signals, because of the dilution of fresh catalysts with this inert material, as well as the presence of embedded products in the catalyst bed formed during the reaction. SiC signals arise in all catalyst XRD patterns, at $2\theta = 34.1, 35.7, 38.0, 41.5, 54.6, 60.12$ and 65.6° . Despite this, different phases of iron have been identified. Except for FeKMo, all diffractograms show a characteristic metallic iron signal at $2\theta = 45.3^\circ$. Iron carbides were identified in all samples, with diffraction peaks between 40 and 50° . Magnetite diffraction peaks were only observed in Fe and FeKMo sample. Characteristic signals of hematite were not detected, indicating that it was reduced and/or carburized during the activation (in active catalysts) to magnetite and then to metallic iron which forms iron carbide rapidly [32]. This results, indicate that the activated catalysts are still in an active form after 60h in stream (carburized and continue being active). The diffraction peak detected at $2\theta = 22^\circ$ in all samples can be attributed to the presence of n-paraffin formed during reaction [33]. Coke phases were not detected.

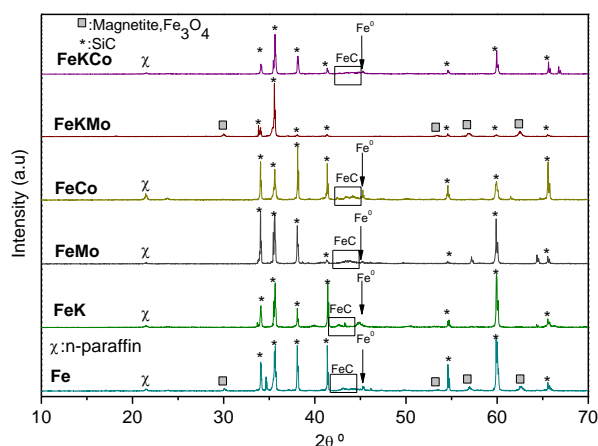


Fig. 7. XRD patterns of Fe-based catalysts after reaction.

4. CONCLUSIONS

In this study, Fe-based catalysts were prepared by precipitation and impregnation to determine the effect of chemical promoters in the production of jet biofuel by FTS. It has been found evidences of the influence of the promoters studied in this work on the catalyst reducibility and carburization. As a consequence Co or K addition seems to stabilize FTS activity as well as to produce an increase in the selectivity increase towards heavier hydrocarbons. A synergistic effect was observed on the Co and K co-promoted catalyst (FeKCo) which shows the best activity and the maximum production of kerosene, as well as gasoline. Molybdenum addition inhibited the reduction and carburization of Fe_2O_3 , maybe due to the formation of a reductant resistant layer on Fe phase. Thus, low FTS activity was observed for this catalyst. A worse result was found in the case of FeKMo, since it was completely inactive in FTS, due to the inhibition of carburization and the formation of Fe_3O_4 . The catalyst behaviour is affected by the species formed during the activation and FTS reaction. After 60h on stream iron carbide phases were detected on Fe, FeK, FeMo, FeCo and FeKCo catalysts, all active in the FTS tests.

Acknowledgements

Financial support from the Spanish Government (CTQ2013-44447-R) and the Regional Government of Madrid

(S2013/MAE-2882) is gratefully acknowledged.

References

- [1] U.S. Energy Information Administration, International Energy Outlook 2016, 2016.
- [2] R.C. Duncan, Big jump in ultimate recovery would ease, not reverse, postpeak production decline, *Oil Gas J.* 102 (2004) 18–21.
- [3] D. Chiamonti, M. Prussi, M. Buffi, D. Tacconi, Sustainable bio kerosene: Process routes and industrial demonstration activities in aviation biofuels, *Appl. Energy.* 136 (2014) 767–774.
- [4] A. de Klerk, Fischer–Tropsch refining: technology selection to match molecules, *Green Chem.* 10 (2008) 1249.
- [5] M.J. a Tijmensen, a. P.C. Faaij, C.N. Hamelinck, M.R.M. Van Hardeveld, Exploration of the possibilities for production of Fischer Tropsch liquids and power via biomass gasification, *Biomass and Bioenergy.* 23 (2002) 129–152.
- [6] P. Lv, Z. Yuan, C. Wu, L. Ma, Y. Chen, N. Tsubaki, Bio-syngas production from biomass catalytic gasification, *Energy Convers. Manag.* 48 (2007) 1132–1139.
- [7] M. Lindo, A.J. Vizcaíno, J.A. Calles, A. Carrero, Ethanol steam reforming on Ni/Al-SBA-15 catalysts: Effect of the aluminium content, *Int. J. Hydrogen Energy.* 35 (2010) 5895–5901.
- [8] A. Carrero, J. Calles, L. García-Moreno, A. Vizcaíno, Production of Renewable Hydrogen from Glycerol Steam Reforming over Bimetallic Ni-(Cu,Co,Cr) Catalysts Supported on SBA-15 Silica, *Catalysts.* 7 (2017) 55.
- [9] R. Sanz, J.A. Calles, D. Alique, L. Furones, H₂ production via water gas shift in a composite Pd membrane reactor prepared by the pore-plating method, *Int. J. Hydrogen Energy.* 39

- (2014) 4739–4748.
- [10] B.Y.F. Morales, B.M. Weckhuysen, Promotion Effects in Co-based Fischer – Tropsch Catalysis, *Catalysis*. 19 (2006) 1–40.
- [11] K. Mai, T. Elder, L.H. Groom, J.J. Spivey, Fe-based Fischer Tropsch synthesis of biomass-derived syngas: Effect of synthesis method, *Catal. Commun.* 65 (2015) 76–80.
- [12] S. Abelló, D. Montané, Exploring iron-based multifunctional catalysts for fischer-tropsch synthesis: A review, *ChemSusChem*. 4 (2011) 1538–1556.
- [13] M. Luo, R.J. O’brien, S. Bao, B.H. Davis, Fischer-Tropsch synthesis: Induction and steady-state activity of high-alpha potassium promoted iron catalysts, *Appl. Catal. A Gen.* 239 (2003) 111–120.
- [14] K. Jothimurugesan, S.K. Gangwal, Titania-Supported Bimetallic Catalysts Combined with HZSM-5 for Fischer - Tropsch Synthesis, *Ind. Eng. Chem. Res.* 37 (1998) 1181–1188.
- [15] V.R. Calderone, N.R. Shiju, D.C. Ferré, G. Rothenberg, Bimetallic catalysts for the Fischer–Tropsch reaction, *Green Chem.* 13 (2011) 1950.
- [16] A. Abbasi, M. Ghasemi, S. Sadighi, Effect of Lanthanum as a Promoter on Fe-Co/SiO₂ Catalyst for Fischer-Tropsch Synthesis, *Bull. Chem. React. Eng. Catal.* 9 (2014) 23–27.
- [17] W. Ma, E.L. Kugler, D.B. Dadyburjor, Effect of Mo loading and support type on hydrocarbons and oxygenates produced over Fe-Mo-Cu-K catalysts supported on activated carbons, *Stud. Surf. Sci. Catal.* 163 (2007) 125–140.
- [18] W. Ma, E.L. Kugler, J. Wright, D.B. Dadyburjor, Mo-Fe catalysts supported on activated carbon for synthesis of liquid fuels by the Fischer-Tropsch process: Effect of Mo addition on reducibility, activity, and hydrocarbon selectivity, *Energy and Fuels*. 20 (2006) 2299–2307.
- [19] S. Qin, C. Zhang, J. Xu, B. Wu, H. Xiang, Y. Li, Effect of Mo addition on precipitated Fe catalysts for Fischer-Tropsch synthesis, *J. Mol. Catal. A Chem.* 304 (2009) 128–134.
- [20] S.C. Ndlela, B.H. Shanks, Reducibility of potassium-promoted iron oxide under hydrogen conditions, *Ind. Eng. Chem. Res.* 42 (2003) 2112–2121.
- [21] A. J. D. Jonge, J. a Moulijn, Temperature-Programmed Reduction of MOO₃ and MOO₂, *J. Phys. Chem.* 89 (1985) 4517–4526.
- [22] M. Shimokawabe, R. Furuichi, T. Ishii, Influence of the Preparation History of α -Fe₂O₃ on Its Reactivity for Hydrogen Reduction, *Thermochim. Acta.* 28 (1979) 287–305.
- [23] H. Hayakawa, H. Tanaka, K. Fujimoto, Preparation of a new precipitated iron catalyst for Fischer-Tropsch synthesis, *Catal. Commun.* 8 (2007) 1820–1824.
- [24] H. Hayakawa, H. Tanaka, K. Fujimoto, Preparation of a new precipitated iron catalyst for Fischer-Tropsch synthesis, *Catal. Commun.* 8 (2007) 1820–1824.
- [25] A. Machocki, Formation of carbonaceous deposit and its effect on carbon monoxide hydrogenation on iron-based catalysts, *Appl. Catal.* 70 (1991) 237–252.
- [26] G. Van Der Laan, a Beenackers, Kinetics and Selectivity of the Fischer–Tropsch Synthesis: A Literature Review, *Catal. Rev.* 41 (1999) 255–318.
- [27] R.A. Dictor, A.T. Bell, Fischer-Tropsch synthesis over reduced and unreduced iron oxide catalysts, *J. Catal.* 97 (1986) 121–136.
- [28] M.E. Dry, Catalytic aspects of industrial Fischer-Tropsch synthesis, *J. Mol. Catal.* 17 (1982) 133–144.
- [29] D.G. Miller, M. Moskovits, A study of the effect of potassium addition to supported iron catalyst in the Fischer-Tropsch reaction, *J. Phys. Chem.* 92 (1988) 6081–6085.
- [30] F.E.M. Farias, F.A.N. Fernandes, F.G. Sales, Effect of operating conditions on fischer-tropsch liquid products produced by unpromoted and

- potassium-promoted iron catalyst, *Lat. Am. Appl. Res.* 40 (2010) 161–166.
- [31] H. Arai, K. Mitsuishi, T. Seiyama, TiO₂-supported Fe-Co, Co-Ni and Ni-Fe alloy catalysts for Fisher-Tropsch Synthesis, *Chem. Lett.* (1984) 1291–1294.
- [32] H.H. Storch, The Fischer-Tropsch and Related Processes for Synthesis of Hydrocarbons by Hydrogenation of Carbon Monoxide, *Adv. Catal.* 1 (1948) 115–156.
- [33] S.M. Rodulfo-Baechler, S.L. González-Cortés, J. Orozco, V. Sagredo, B. Fontal, A.J. Mora, G. Delgado, Characterization of modified iron catalysts by X-ray diffraction, infrared spectroscopy, magnetic susceptibility and thermogravimetric analysis, *Mater. Lett.* 58 (2004) 2447–2450.